

Accepted Manuscript

Ferrocene containing *N*-tosyl hydrazones as optical and electrochemical sensors for Hg^{2+} , Cu^{2+} and F^{-} ions

Li Ling, Jianfeng Hu, Hao Zhang



PII: S0040-4020(19)30298-4

DOI: <https://doi.org/10.1016/j.tet.2019.03.023>

Reference: TET 30209

To appear in: *Tetrahedron*

Received Date: 27 December 2018

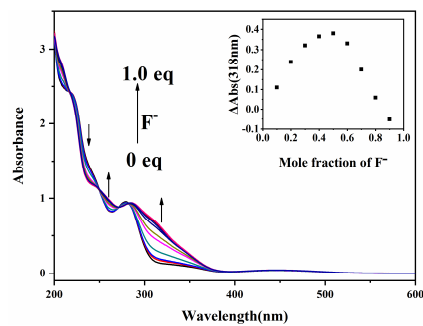
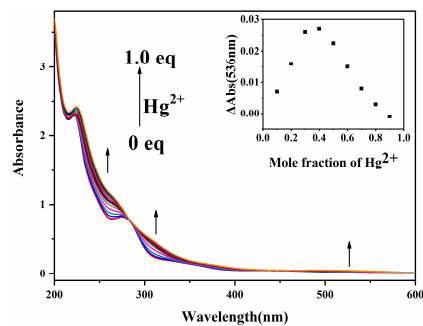
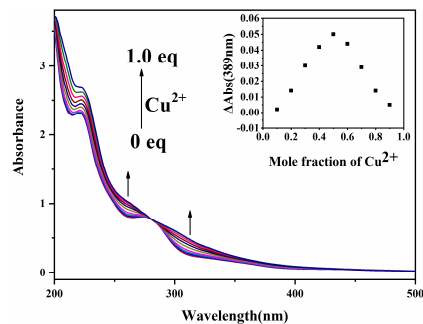
Revised Date: 8 March 2019

Accepted Date: 11 March 2019

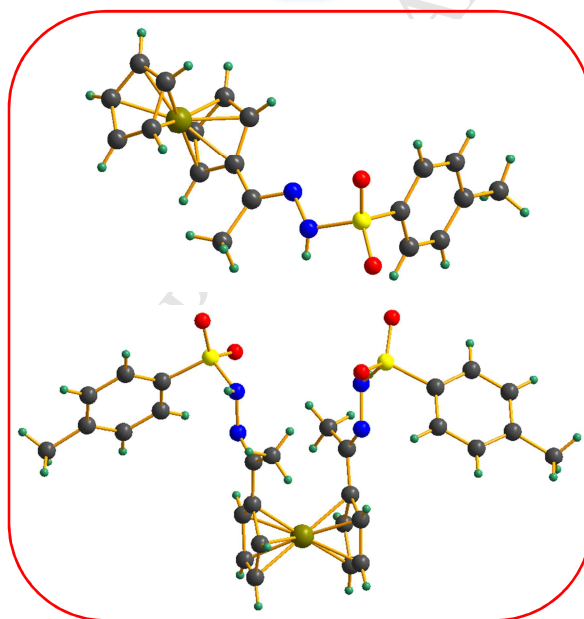
Please cite this article as: Ling L, Hu J, Zhang H, Ferrocene containing *N*-tosyl hydrazones as optical and electrochemical sensors for Hg^{2+} , Cu^{2+} and F^{-} ions, *Tetrahedron* (2019), doi: <https://doi.org/10.1016/j.tet.2019.03.023>.

This is a PDF file of an unedited manuscript that has been accepted for publication. As a service to our customers we are providing this early version of the manuscript. The manuscript will undergo copyediting, typesetting, and review of the resulting proof before it is published in its final form. Please note that during the production process errors may be discovered which could affect the content, and all legal disclaimers that apply to the journal pertain.

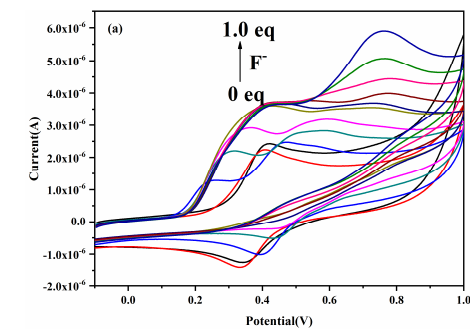
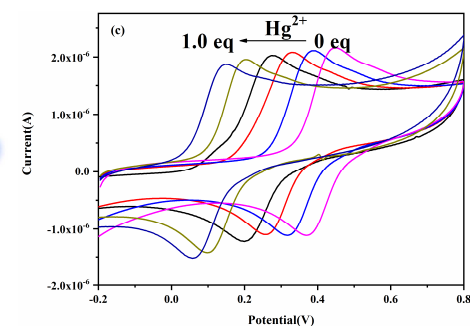
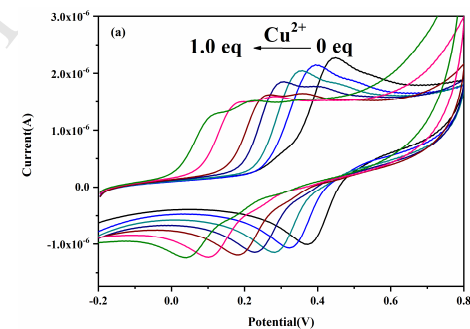
UV-vis changes



Colorimetric changes



Electrochemical changes



Ferrocene Containing *N*-tosyl Hydrazones as Optical and Electrochemical Sensors for Hg^{2+} , Cu^{2+} and F^- Ions

Li Ling^{a,b}, Jianfeng Hu^{a,b}, Hao Zhang^{a,b,c} *

^a College of Chemistry & Chemical Engineering, Inner Mongolia University, Hohhot 010021, P. R. China.

^b Inner Mongolia Key Laboratory of Fine Organic Synthesis, Hohhot 010021, P. R. China.

^c State Key Laboratory of Polymer Physics and Chemistry, Changchun Institute of Applied Chemistry, Chinese Academy of Sciences, Changchun 130022, P. R. China

Keywords: ferrocene, hydrazone, optical signal, electrochemical signal

Abstract

Ferrocene containing *N*-tosyl hydrazones as selective and sensitive optical and electrochemical chemosensors were synthesized and characterized by ^1H NMR, ^{13}C NMR, ESI-MS and X-ray analysis. The cation and anion binding studies were carried out using various techniques including electrochemistry, UV-vis and ^1H NMR spectroscopy. Chemosensors **2a** and **2b** have shown excellent selective recognition toward Hg^{2+} , Cu^{2+} and F^- through optical and electrochemical signals. The colour of **2a** and **2b** in solution changed visibly from pale yellow to red upon addition of Hg^{2+} ion, while the color of solution changed from pale yellow to yellow green upon addition of Cu^{2+} , which can be easily detected by the naked eye.

1 Introduction

Heavy metals are found naturally in the earth.¹ They become concentrated as a result of human caused activities and can enter plant, animal, and human tissues via inhalation, diet, and manual handling.² Among the heavy metals, mercury is one of the most toxic metal ions and is widely used in industry, such as coal mining, wood pulping, and chemical manufacturing, and in other products of daily life. It can be easily absorbed and accumulated from the environment by living organisms and causes DNA damages, mitosis impairment, central nervous and endocrine systems disruption.³ In addition, copper is essential to human health as a trace dietary mineral.⁴

* Corresponding author at: College of Chemical & Chemical Engineering, Inner Mongolia University, Hohhot 010021, P. R. China.

E-mail addresses: haozhang@imu.edu.cn, zh_hjf@hotmail.com (H. Zhang).

However, the excess Cu^{2+} ion may cause several neurological diseases, such as Parkinson's disease, epileptic seizures, kidney and liver damages.⁵ On the other hand, amongst potential anions of environmental concern, fluoride is one of particular important biologically functional anions owing to its established role in dental care⁶ and treatment of Osteoporosis⁷. While excessive use may cause fluorosis resulting in the discoloration of teeth.^{8,9}

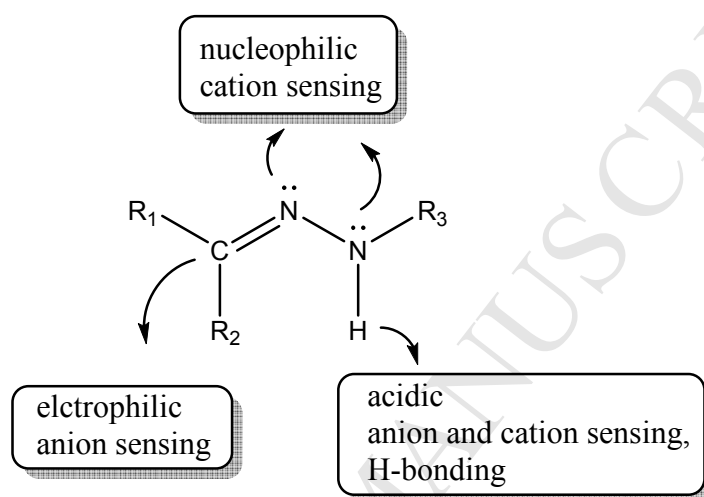


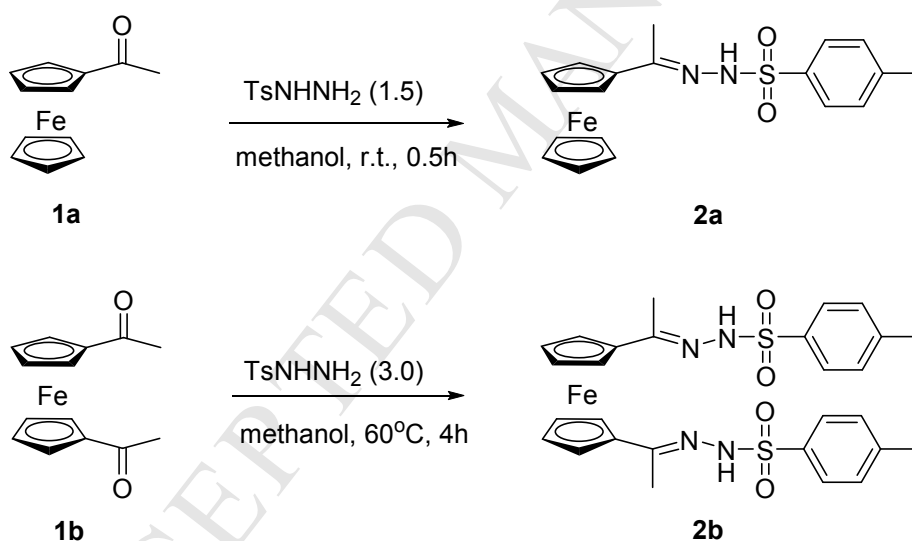
Fig. 1. The structure of the hydrazone group.

Therefore, selective detection and sensing mercury, copper and fluoride ions have received much attention from the scientific community. One of the most elegant ways of achieving sensor design is to functionalize a receptor with selective recognition units and physical signal response units (redox shifts, color changes and fluorescence quenching or enhancement). Ferrocene unit is often applied to redox sensors due to its unique electrochemical properties and easy functionalization.^{10,11} Recently, hydrazone functional group has proved to be a versatile ion recognition unit for both cations and anions,¹²⁻²² since the functional diversity of its structure. As shown in Figure 1 the nucleophilic nitrogen atom, electrophilic imine carbon, and acidic N-H proton, enables its use in highly sensitive and selective sensor of cations, anions, and even neutral molecules. However, chemosensors combining ferrocene and hydrazone functional groups are rarely investigated.²³⁻²⁵ Herein, ferrocene containing *N*-tosyl hydrazones **2a** and **2b** have been synthesized and its capability of optical and redox sensing of cations and anions has been demonstrated.

2. Results and discussion

2.1. Synthesis and characterization

Ferrocene containing *N*-tosyl hydrazones **2a** and **2b** were prepared according to the literature procedures.²⁶ As shown in Scheme 1, acetyl ferrocene **1a** and 1,1'-diacetyl-ferrocene **1b** reacted with *p*-toluenesulfonyl hydrazide in methanol to give compound **2a** and **2b** in 86% and 80% yields, respectively. (Scheme 1). Compounds **2a** and **2b** were characterized by ¹H NMR, ¹³C NMR and HRMS (ESI-TOF). In addition, the structure of compound **2a** and **2b** were also confirmed by single-crystal X-ray diffraction analysis (Figure 2 and 3). The cations and anions recognition properties of the chemosensors have been established by UV-vis spectroscopy, electrochemistry and ¹H NMR titration.



Scheme 1. Synthesis of ferrocene containing *N*-tosyl hydrazone.

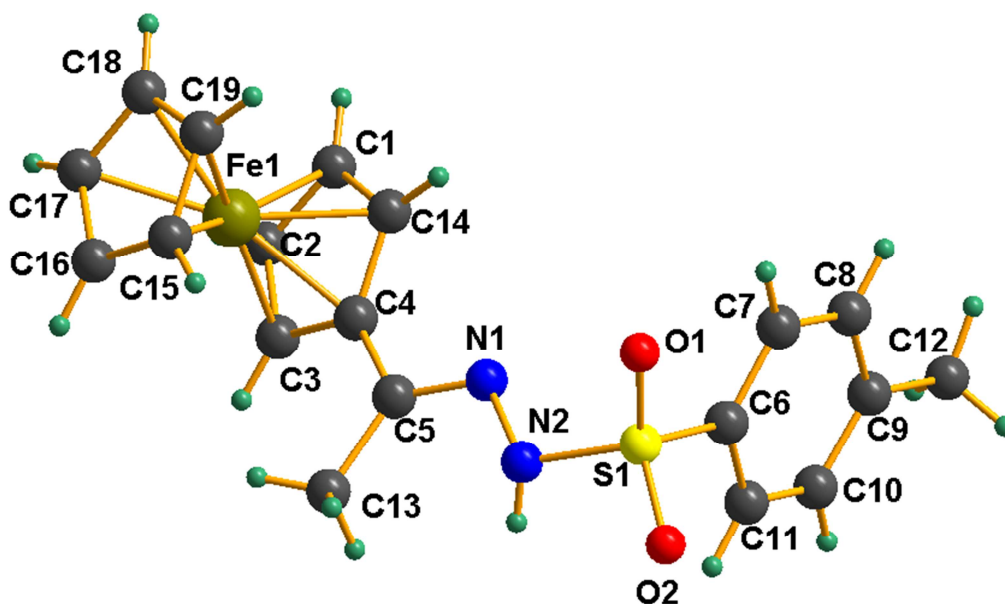


Fig. 2. Molecular structure of **2a**. Selected bond lengths (Å) and angles (deg): N1-C5 = 1.286(4), N1-N2 = 1.417(3), S1-N2 = 1.635(3), S1-O1 = 1.420(2), S1-O2 = 1.443(2), S1-C6 = 1.749(4); N1-C5-C4 = 116.3(3), C5-N1-N2 = 113.5(2), N1-N2-S1 = 114.1(2), N2-S1-C6 = 108.40(14), O1-S1-N2 = 108.56(15), O2-S1-N2 = 103.18(14).

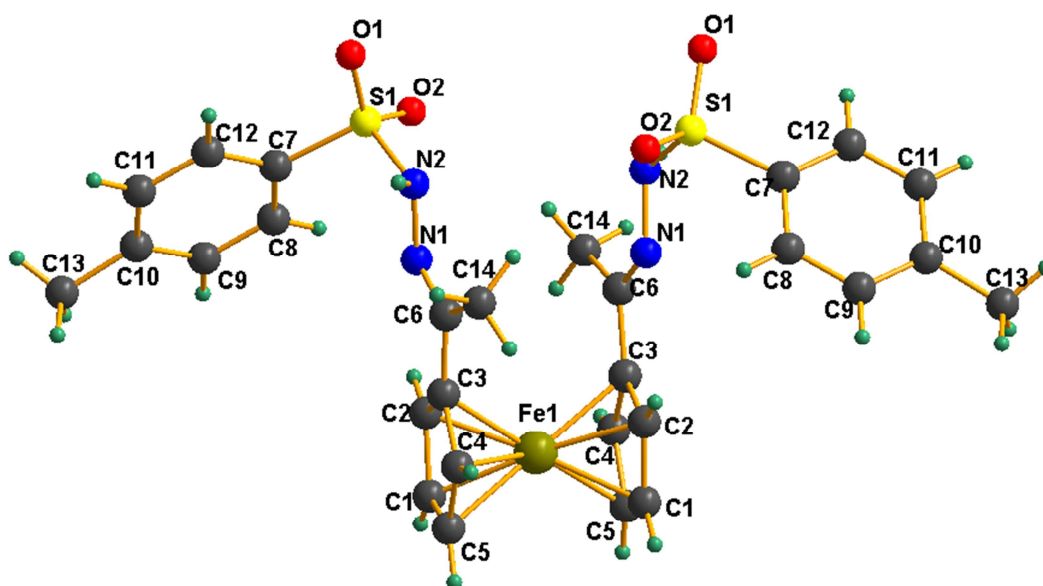


Fig. 3. Molecular structure of **2b**. Selected bond lengths (Å) and angles (deg): N1-C6 = 1.276(8), N1-N2 = 1.411(7), S1-N2 = 1.643(5), S1-O1 = 1.440(5), S1-O2 = 1.429(7), S1-C7 = 1.756(6); N1-C6-C14 = 125.0(6), C6-N1-N2 = 115.9(5), N1-N2-S1 = 111.5(4), N2-S1-C7 = 107.1(3), O1-S1-N2 = 104.6(3), O2-S1-N2 = 107.3(3).

2.2. UV-vis absorption studies

The UV-vis spectrum of **2a** and **2b** (Figure 4) in CH₃CN (1×10^{-4} M) exhibits high-energy (HE) absorption bands at 280 nm, produced by π - π^* charge transfer (CT) transition of the phenyl group, and low energy (LE) absorption band at 445nm corresponds to ferrocene-centered metal-to-ligand charge transfer (MLCT). The UV-vis binding interaction studies of **2a** and **2b** in CH₃CN (1×10^{-4} M) against cations such as Li⁺, Na⁺, K⁺, Mg²⁺, Ca²⁺, Fe²⁺, Co²⁺, Ni²⁺, Cu²⁺, Zn²⁺, Pb²⁺, Cd²⁺, Ag⁺ and Hg²⁺ as perchlorate salts, showed selective response to Cu²⁺ and Hg²⁺ (Figure 4).

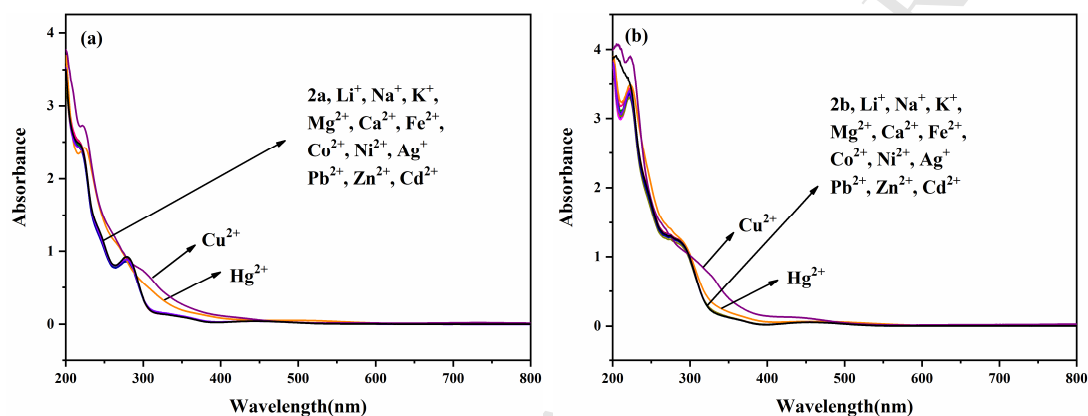
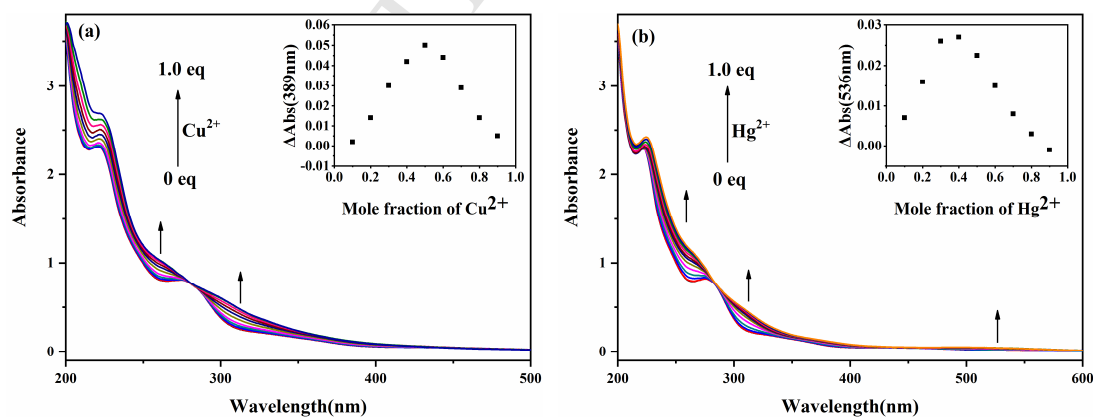


Fig. 4. (a) UV-vis absorption spectra of chemosensor **2a** observed upon addition of 1 equiv. of various metal ions in CH₃CN (1×10^{-4} M). (b) UV-vis absorption spectra of chemosensor **2b** observed upon addition of 1 equiv. of various metal ions in CH₃CN (1×10^{-4} M).



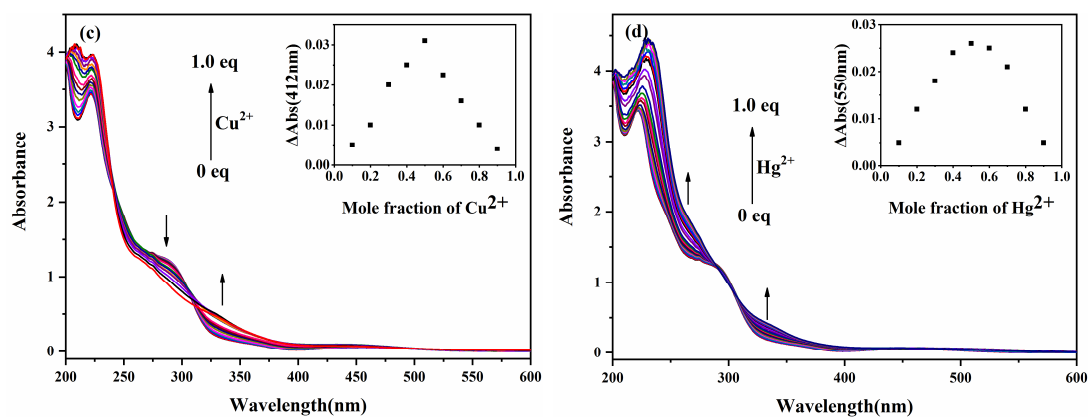


Fig. 5. UV-vis absorption titration spectra of chemosensor **2a** with Cu(ClO₄)₂(a) and Hg(ClO₄)₂(b) in CH₃CN (1×10⁻⁴ M); UV-vis absorption titration spectra of chemosensor **2b** with Cu(ClO₄)₂(c) and Hg(ClO₄)₂(d) in CH₃CN (1×10⁻⁴ M).

The change in the UV-vis absorbance spectra of **2a** in CH₃CN due to the stepwise addition of Cu²⁺ and Hg²⁺ ion are shown in Figure 4a and b. Upon addition of Cu²⁺ (Figure 5a), absorption band at 445nm decreased and absorption band from 550-800 nm increased, with a color change from pale yellow to yellow green (Figure 6). While after addition of 1 equiv. of Hg²⁺ (Figure 5b), absorption band at 445nm increased with a 65 nm red shift, which is accountable for the change of color from pale yellow to red (Figure 6). Motivated by the obvious color changes of **2a** to Cu²⁺ and Hg²⁺ in CH₃CN, visual test paper was prepared. Changes in color from pale yellow to orange red and pale yellow to yellow green were immediately observed by naked eye on the test paper after addition of Hg²⁺ and Cu²⁺ ions in water (1×10⁻³ M) followed by the addition of dropwise of CH₃CN (Figure S30).



Fig. 6. Visual color changes of chemosensor **2a** upon addition of various metal ions (1 equiv.) in CH₃CN (1×10⁻⁴ M).

During the titration of Cu^{2+} to **2b**, a well defined isosbestic points were observed at 300 nm. This is indicative of the presence of the complexing equilibrium of **2b** with Cu^{2+} . Meanwhile absorption band at 283 nm decreased with a concomitant increase of absorption band at 350 nm (Figure 5c). When the titration of Hg^{2+} to **2b**, intensity of absorption band at 283 nm and 350 nm enhanced concurrently (Figure 5d).

Binding assays using the method of continuous variations (Job's plot) are consistent with a 1:1 stoichiometry in **2a**/ Cu^{2+} , **2b**/ Cu^{2+} and **2b**/ Hg^{2+} complexes (Figure 5a, 5c and 5d, inset). Job's plot of **2a** with Hg^{2+} indicated the formation of 2:1 complexes (Figure 5b, inset). This result has also been confirmed by ESI-MS, where a peaks at m/z 458.9882 for [**2a**+ Cu^{2+}], m/z 993.0837 for [**2a**+**2a**+ Hg^{2+} - H^+], m/z 669.0401 for [**2b**+ Cu^{2+}] and m/z 807.0682 for [**2b**+ Hg^{2+} - H^+], were observed. Following the Benesi-Hildebrand equation,^{27,28} the apparent binding constants were observed to be $9.90 \times 10^3 \text{ M}^{-1}$ for **2a**- Cu^{2+} , $2.3 \times 10^{13} \text{ M}^{-1}$ for **2a**- Hg^{2+} , $3.2 \times 10^3 \text{ M}^{-1}$ for **2b**- Cu^{2+} and $4.4 \times 10^3 \text{ M}^{-1}$ for **2b**- Hg^{2+} (Figure S13 and S15). Detection limits could reach $2.66 \times 10^{-5} \text{ M}$ for **2a**- Cu^{2+} , $7.60 \times 10^{-6} \text{ M}$ for **2a**- Hg^{2+} , $3.55 \times 10^{-5} \text{ M}$ for **2b**- Cu^{2+} and $3.06 \times 10^{-5} \text{ M}$ for **2b**- Hg^{2+} (Figure S14 and S16).

The anion binding properties of receptors **2a** and **2b** were investigated using UV-visible studies. When a set of anions (OAc^- , NO_3^- , HSO_4^- , H_2PO_4^- , F^- , Cl^- , Br^- , as TBA^+ salts) were added to the solution of **2a** and **2b** ($1 \times 10^{-4} \text{ M}$) in CH_3CN , only F^- promote remarkable spectral changes (Figure 7). The changes in the UV-vis absorbance spectra of **2a** and **2b** due to the stepwise addition of F^- ion are shown in Figure 8. After the addition of 1 equiv. of F^- , the absorption bands at 350 nm increased. Binding assays using the method of continuous variations (Job's plot) suggest a 1:1 binding model for receptor/anion stoichiometry, with binding constants $K = 1.0 \times 10^4 \text{ M}^{-1}$, $K = 1.7 \times 10^3 \text{ M}^{-1}$, in the cases of **2a** and **2b**, respectively (Figure S17). Detection limits could reach $1.64 \times 10^{-5} \text{ M}$ for **2a**- F^- and $1.91 \times 10^{-5} \text{ M}$ for **2b**- F^- (Figure S18).

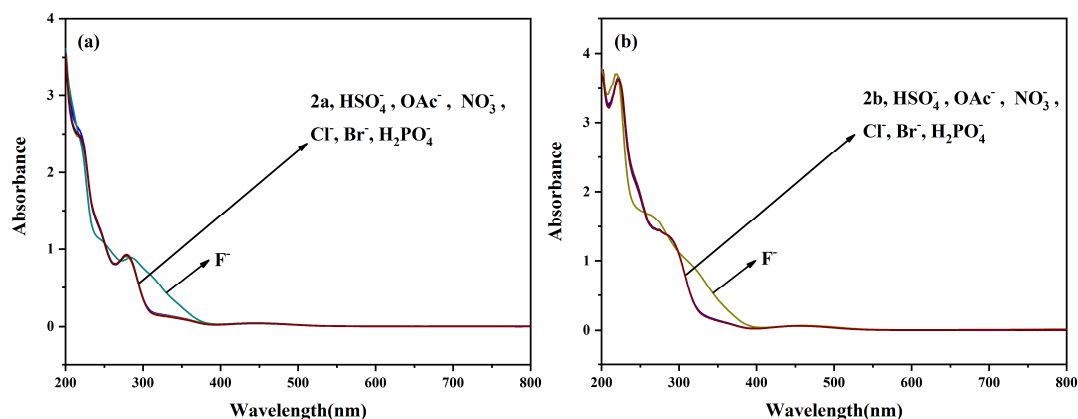


Fig. 7. (a) UV-vis absorption spectra of chemosensor **2a** observed upon addition of 1 equiv. of various anions in CH_3CN (1×10^{-4} M). (b) UV-vis absorption spectra of chemosensor **2b** observed upon addition of 1 equiv. of various anions in CH_3CN (1×10^{-4} M).

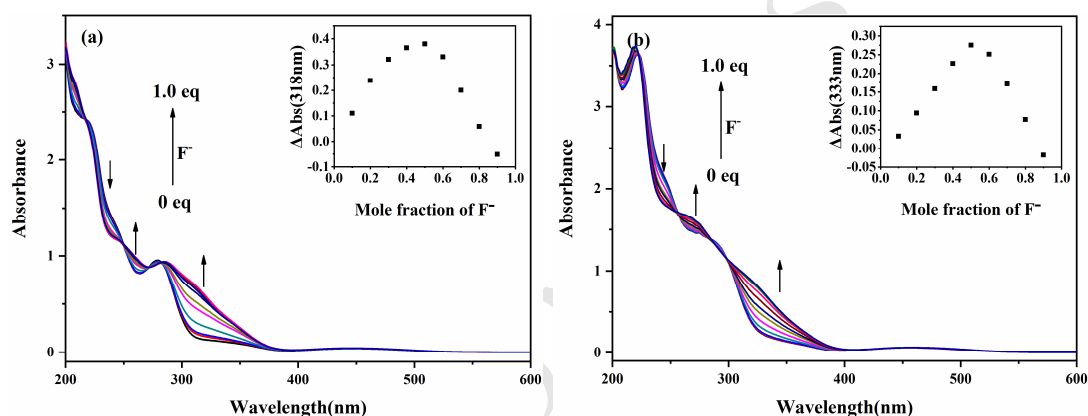


Fig. 8. UV-vis absorption titration spectra of chemosensors **2a** (a) and **2b** (b) with F^- in CH_3CN (1×10^{-4} M).

The competitive experiments in the presence of Cu^{2+} and Hg^{2+} ions mixed with 1 equivalent of Li^+ , Na^+ , K^+ , Mg^{2+} , Ca^{2+} , Fe^{2+} , Co^{2+} , Ni^{2+} , Zn^{2+} , Pb^{2+} , Cd^{2+} and Ag^+ ions were carried out. As shown in Figure S31 and Figure S32, no significant variations in the UV-vis absorbance spectra were obtained. While both of Cu^{2+} and Hg^{2+} ions are present in the solution, only Cu^{2+} ion can be detected from the UV-vis signal (Figure S33). Specificity of anion detection is evaluated by adding interfering anions (OAc^- , NO_3^- , HSO_4^- , H_2PO_4^- , Cl^- , Br^-) into F^- solution. As shown in Figure S34, **2a** can be used as an excellent sensor for F^- detection in the presence of the competing anions.

2.3. Electrochemical studies

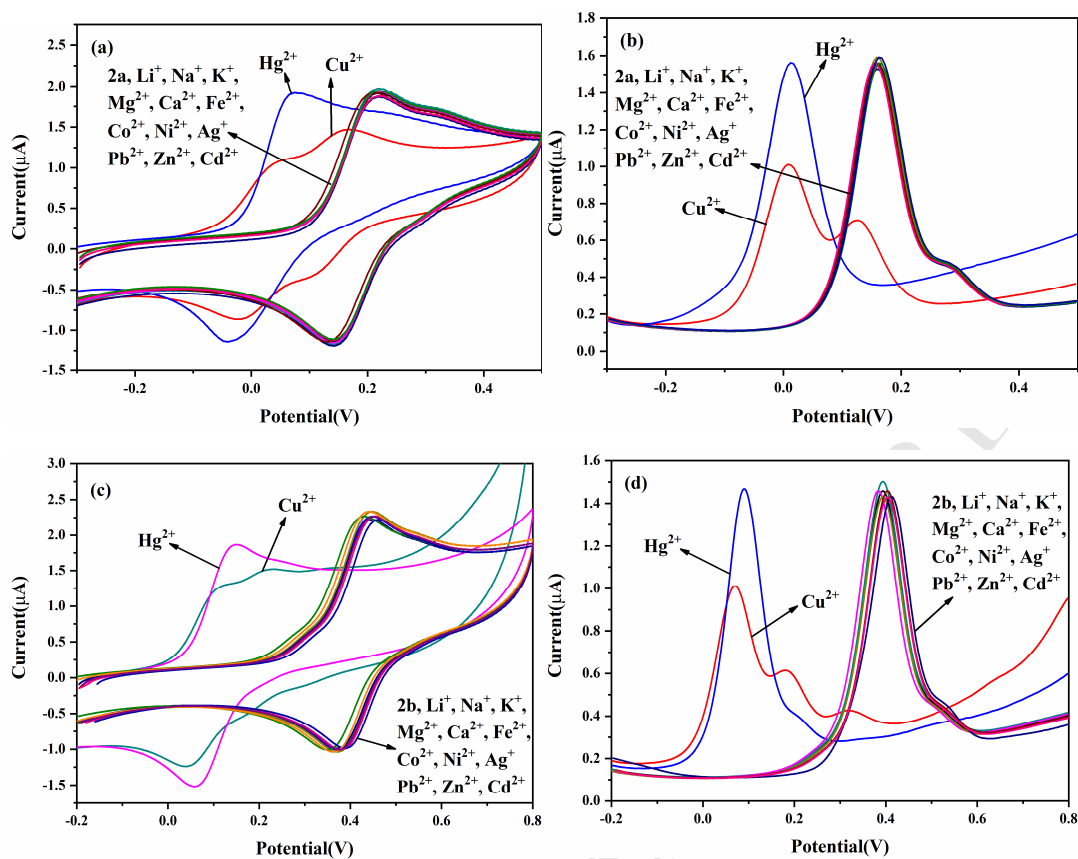
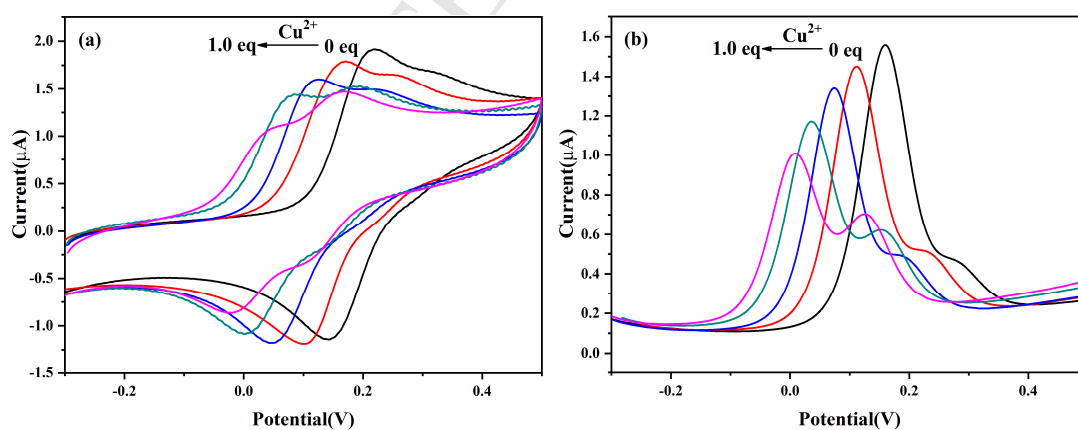


Fig. 9. Cyclic Voltammetry and Differential Pulse Voltammetry spectra of **2a** (a), (b) and **2b** (c), (d) observed upon addition of 1 equiv of various metal ions in CH₃CN (100 μM), containing 0.1 M [(n-C₄H₉)₄NPF₆] as supporting electrolyte.



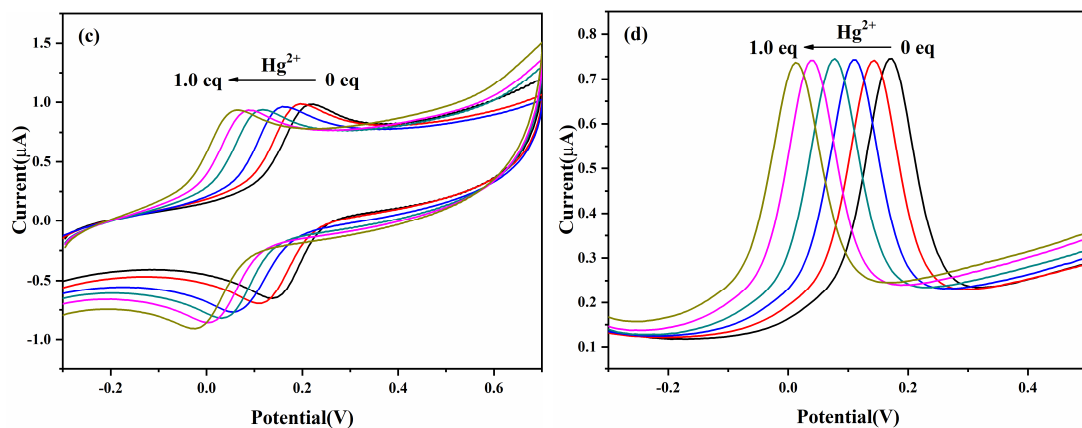


Fig. 10. Cyclic Voltammetry and Differential Pulse Voltammetry of chemosensor **2a** with $\text{Cu}(\text{ClO}_4)_2$ (a), (b) and $\text{Hg}(\text{ClO}_4)_2$ (c), (d) in CH_3CN (1×10^{-4} M), containing 0.1 M $[(n\text{-C}_4\text{H}_9)_4\text{NPF}_6]$ as supporting electrolyte.

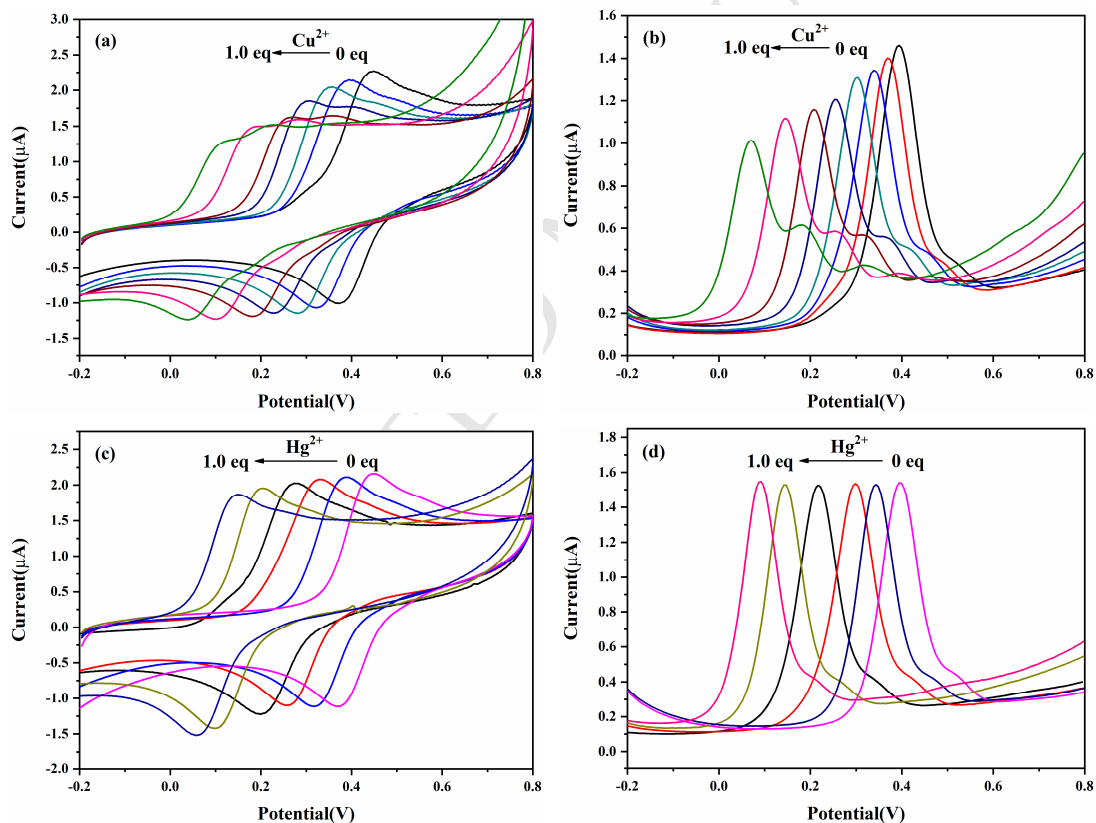


Fig. 11. Cyclic Voltammetry and Differential Pulse Voltammetry of chemosensor **2b** with $\text{Cu}(\text{ClO}_4)_2$ (a), (b) and $\text{Hg}(\text{ClO}_4)_2$ (c), (d) in CH_3CN (1×10^{-4} M), containing 0.1 M $[(n\text{-C}_4\text{H}_9)_4\text{NPF}_6]$ as supporting electrolyte.

The metal recognition properties of chemosensors **2a** and **2b** were also evaluated by cyclic voltammetry (CV) and differential pulse voltammetry (DPV) analysis in CH₃CN solutions containing 0.1 M [(n-C₄H₉)₄NPF₆] as supporting electrolyte. Compounds **2a** and **2b** both display a reversible one-electron-oxidation process at $E_{1/2} = 0.218$ and 0.446 V, respectively, due to the ferrocene/ferrocenium redox couple. No perturbation of the CV and DPV voltammograms of **2a** and **2b** were observed in the presence of Li⁺, Na⁺, K⁺, Mg²⁺, Ca²⁺, Fe²⁺, Co²⁺, Ni²⁺, Zn²⁺, Cd²⁺, Ag⁺ and Pb²⁺ as their appropriate salts (Figure 9). However, on stepwise addition of Cu²⁺ ion to **2a**, original peak gradually decreased and negatively shifted to $E_{1/2} = -0.041$ V (Figure 10a). While, upon stepwise addition of Hg²⁺ ion to **2a**, a clear evolution of the oxidation wave from $E_{1/2} = 0.218$ to $E_{1/2} = 0.059$ V was observed, and maximum perturbation of the CV was obtained with 1 equiv. of Hg²⁺ ion added (Figure 10c). The DPV of **2a** illustrated the similar results (Figure 10b and d). As for compound **2b**, on stepwise addition of Cu²⁺ ion, a clear shift of the oxidation wave from $E_{1/2} = 0.444$ V to $E_{1/2} = 0.115$ V was observed accompanied by a decrease in current intensity (Figure 11a). When the stepwise addition of Hg²⁺ ion to **2b**, the oxidation peak negatively shifted to $E_{1/2} = 0.146$ V with 1 equiv. of added Hg²⁺ ion (Figure 11c). Changes of the DPV titration experiment of **2b** with Cu²⁺ and Hg²⁺ (Figure 11b and d) confirmed the results of the CV titration experiment.

The recognition behavior of receptor **2a** and **2b** toward anions was also studied by electrochemistry. It was observed that addition of F⁻ to **2a** and **2b** promotes remarkable changes in the redox behavior (Figure 12). On the addition of increasing amounts of F⁻ ions, oxidation peak decreased and shifted anodically accompanied by increasing of two new oxidation peak (Figure 13a, c). It was also observed that in the presence of excess of F⁻ the CV wave of **2a** and **2b** becomes irreversible. The results of the DPV titration experiment matched exactly with that of the CV studies (Figure 13b, d).

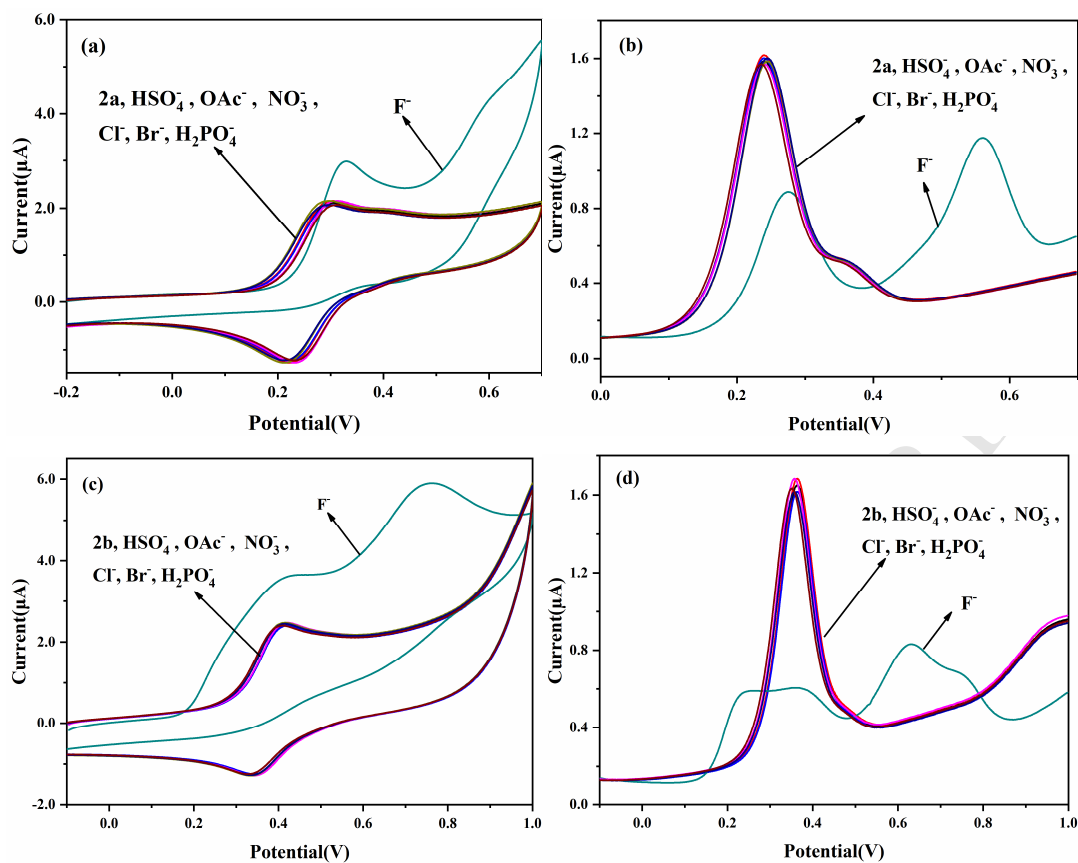
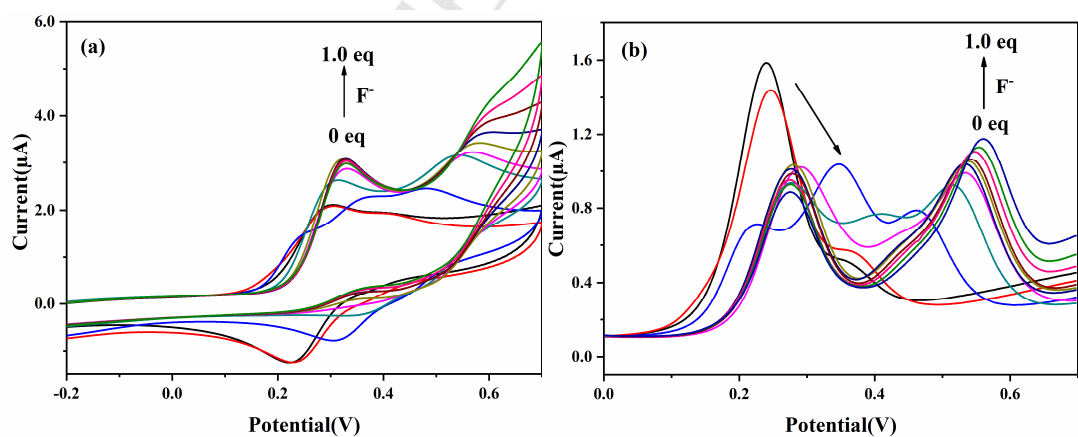


Fig. 12. Cyclic Voltammetry and Differential Pulse Voltammetry spectra of **2a** (a), (b) and **2b** (c), (d) observed upon addition of 1 equiv. of various anions in CH_3CN (100 μM), containing 0.1 M $[(n\text{-C}_4\text{H}_9)_4\text{NPF}_6]$ as supporting electrolyte.



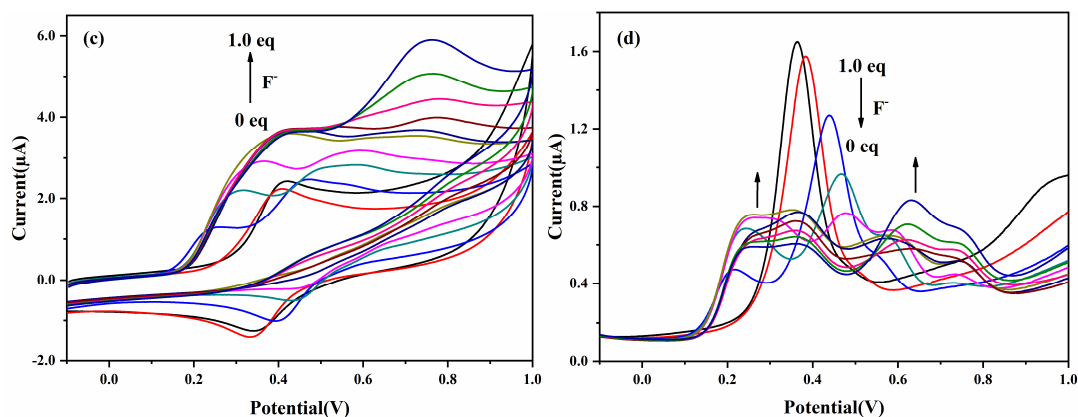


Fig. 13. Cyclic Voltammetry and Differential Pulse Voltammetry of chemosensors **2a** (a), (b) and **2b** (c), (d) with F^- in CH_3CN (1×10^{-4} M), containing 0.1 M $[(n-C_4H_9)_4NPF_6]$ as supporting electrolyte.

2.4. Binding studies.

The binding properties of chemosensor **2a** with Hg^{2+} were evaluated by 1H NMR studies in deuterated DMSO solution (Figure 14). The complexation process induces obvious upfield changes in the chemical shifts in the amino proton Ha ($\Delta\delta = 0.0182$ ppm) and phenyl proton Hb next to sulphone substituent group ($\Delta\delta = 0.0114$ ppm). Meanwhile phenyl proton Hb next to methyl substituent downshifted for 0.0210 ppm. The signal corresponding to methyl group proton Hc and Hd slightly downshifted for 0.0058 ppm and 0.0068 ppm, respectively. The downfield shifts of the cyclopentadienyl ring protons (He, Hf) in ferrocene were observed in smaller magnitude ($\Delta\delta = 0.0028$ -0.0066 ppm). From the magnitude of these observed shifts, it can be surmised that complexation exerts a more powerful effect on the imine group and phenyl group than ferrocene group. The sulphur atom is surrounded with one phenyl group and two oxygen atom, which makes sulphur atom difficult to coordinate with Hg^{2+} . Finally, it can be concluded that the plausible binding mode of Hg^{2+} is the oxygen atom of the sulphone group and N atom of the imine group (Figure 14).

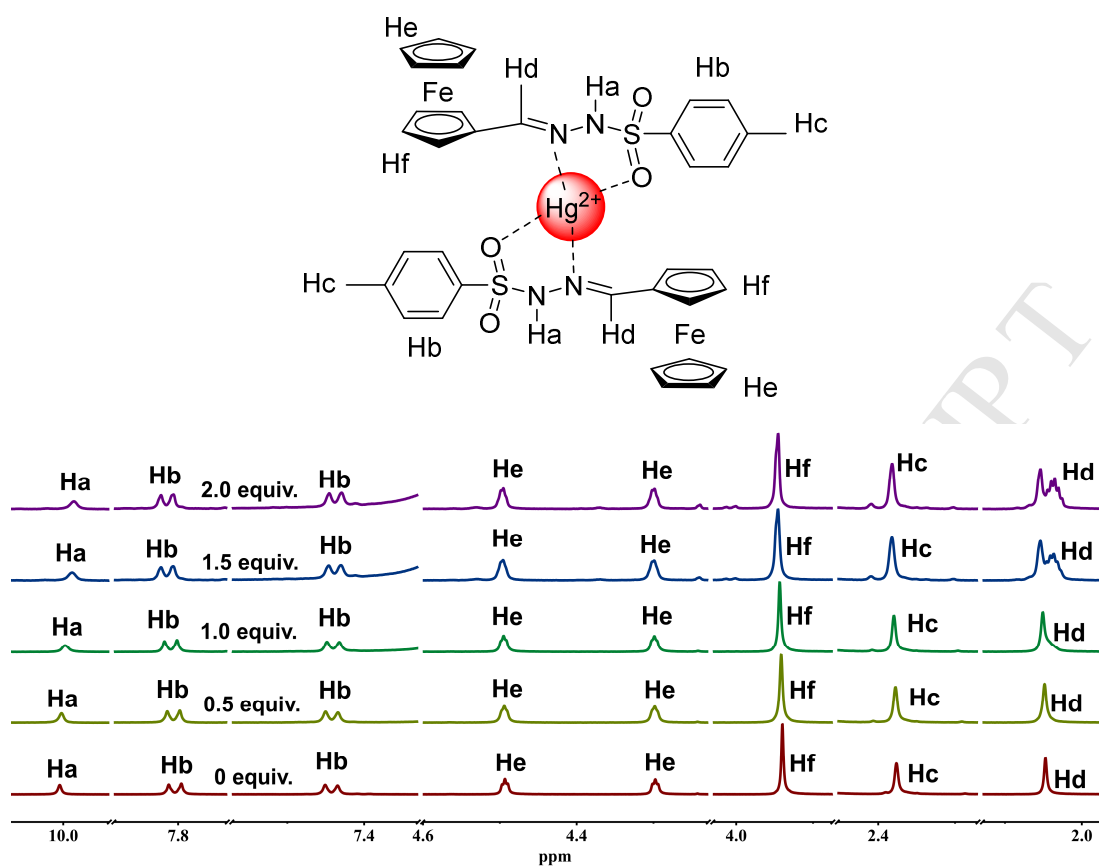


Fig. 14. Evolution of the ^1H NMR spectra of **2a** upon addition of 2.0 equiv. Hg^{2+} in the DMSO solution.

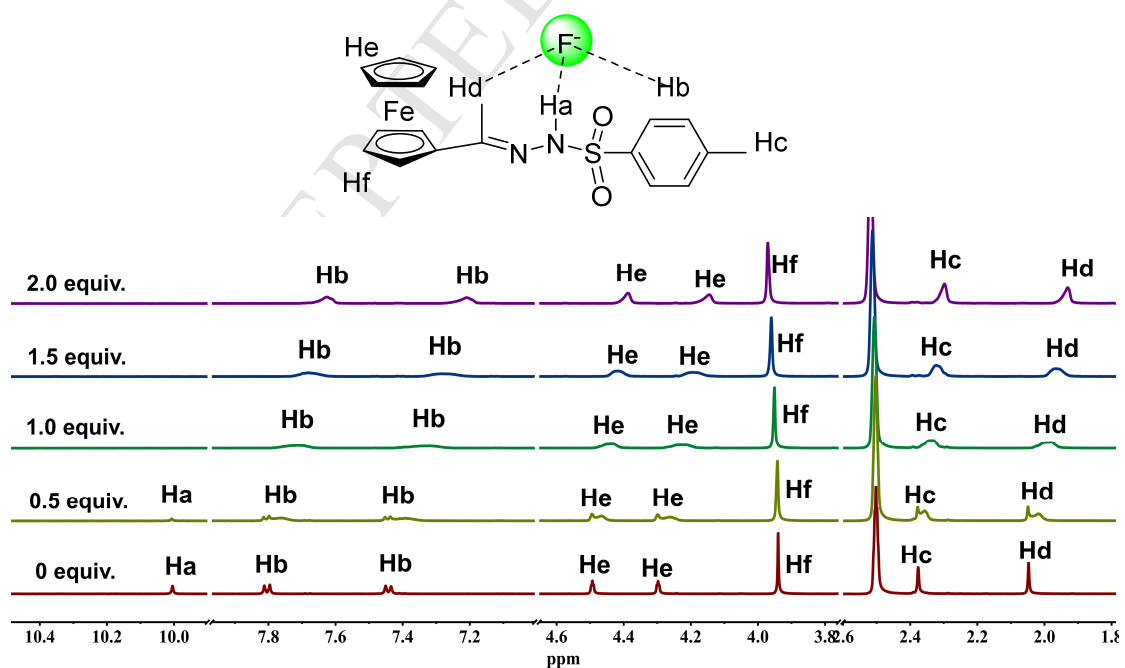


Fig. 15. Evolution of the ^1H NMR spectra of **2a** upon addition of 2.0 equiv. F^- in the DMSO solution.

The binding properties of chemosensor **2a** with F^- were also evaluated by 1H NMR studies in deuterated DMSO solution (Figure 15). The signal for the amine proton Ha exhibited a downfield shift of $\Delta\delta = 0.0022$ ppm on adding 0.5 equivalent of F^- ions. On further addition of 1 equivalent of F^- ions the signal for the Ha proton disappeared, demonstrating that the binding process involve initial formation of H-bond between the amine proton Ha and F^- ions followed by deprotonation. The binding process induces noticeable upfield changes in the chemical shifts of the phenyl ring protons ($\Delta\delta = 0.1773$ ppm) and monosubstituted cyclopentadienyl ring protons ($\Delta\delta = 0.1065, 0.1531$ ppm). Similarly, The signal corresponding to methyl group proton Hc and Hd also got shifted by 0.0784 ppm and 0.1168ppm respectively. From the magnitude of the observed 1H chemical shifts, it can be concluded that the F^- ions have hydrogen bond effect not only with amine protons but also with phenyl protons and methyl protons.

3. Conclusions

In conclusion, we have described new ferrocene containing hydrazones **2a** and **2b** through combining the redox activity of the ferrocene unit with the binding ability of hydrazone, and examined its binding properties towards various guest cations and anions using electrochemical, spectral and optical techniques. Ferrocene containing hydrazones **2a** and **2b** exhibits high binding affinity and sensitivity for Hg^{2+} , Cu^{2+} and F^- ions. The Fc/Fc^+ redox couple was significantly cathodically shifted on complexation with Cu^{2+} and Hg^{2+} . Interestingly, When Hg^{2+} ion was added into the solution of **2a**, **2b** the color changed from pale yellow to red. As for Cu^{2+} ion was added into the solution of **2a** and **2b**, the color changed from pale yellow to yellow green, which allows their potential use for “naked-eye” detection. Moreover, Addition of F^- ions induced changes in UV-vis absorption spectra and electrochemical signals. It has been demonstrated that hydrazones **2a** and **2b** can bind with F^- through H-bonding between hydrazone N-H proton and the F^- as proved by 1H NMR titration.

4 Experimental

4.1. Materials and methods

All reagents were used as received from commercial sources without further purification. All solvents were purified according to literature techniques. For column chromatography, 200–300 mesh silica gel (Qingdao, China) was employed. The cyclic voltammetry (CV) and differential pulse voltammetry (DPV) were performed with a conventional three-electrode configuration consisting of glassy carbon as the working electrode, platinum as an auxiliary electrode and Ag/Ag⁺ as a reference electrode. The concentration of the sample solutions was 100 μM in CH₃CN containing 0.1 M [(n-C₄H₉)₄NPF₆] as supporting electrolyte and the scan rate was 0.1 Vs⁻¹. The UV–vis spectra were carried out in CH₃CN solutions of 100 μM concentration.

4.2. Instrumentation

All NMR experiments were carried out on a Bruker AVANCE 500MHz nuclear magnetic resonance spectrometer using CDCl₃ or DMSO-*d*₆ as the solvent with tetramethylsilane as the internal standard. Chemical shift values (δ) were given in parts per million. HRMS data were obtained on a Bruker QTOF mass spectrometer. The melting points were determined on an X-4 binocular microscope melting point apparatus and uncorrected. The UV–vis absorption spectra were recorded with Shimadzu UV-2700 ultraviolet and visible spectrophotometer. The CV and DPV measurements were carried out on the Autolab PGSTAT302N potentiostat (Metrohm Autolab B. V.). X-ray single-crystal data were collected using Mo Kα (λ = 0.710 73 Å) radiation on a Bruker APEX II diffractometer equipped with a CCD area detector.

4.3. Synthetic procedure

4.3.1 Synthesis of chemosensor **2a**

A solution of pure TsNHNH₂ (15 mmol) in methanol (30 mL) was stirred and heated to 60 °C until the TsNHNH₂ dissolved. The mixture was cooled to room temperature. Then a solution of acetyl ferrocene **1a** (10 mmol) in methanol was dropped into the mixture slowly. After approximately 0.5h, the crude products could be obtained as solid precipitate. The precipitate was washed with petroleum ether then removed in vacuo to give yellow solid **2a** in 86% yield. mp 187-189 °C. ¹H NMR

(500 MHz, DMSO) δ 10.00 (s, 1H), 7.81 (d, $J = 7.9$ Hz, 2H), 7.43 (d, $J = 7.8$ Hz, 2H), 4.49 (s, 2H), 4.29 (s, 2H), 3.93 (s, 5H), 2.36 (s, 3H), 2.04 (s, 3H). ^{13}C NMR (126 MHz, DMSO) δ 155.1, 143.0, 136.4, 129.1, 127.6, 69.6, 68.9, 66.8, 20.9, 15.0. HRMS (ESI-TOF) m/z : $[\text{M}]^+$ calcd. for $\text{C}_{19}\text{H}_{20}\text{FeN}_2\text{O}_2\text{S}$ 396.0595; Found: 396.0594.

4.3.2 Synthesis of chemosensor **2b**

A solution of pure TsNHNH_2 (30 mmol) in methanol (60 mL) was stirred and heated to 60 °C until the TsNHNH_2 dissolved. Then, 1,1'- diacetyl- ferrocene (10 mmol) was added into the mixture slowly. After refluxing for 4 h, the crude product could be obtained as solid precipitate. The precipitate was washed with petroleum ether then removed in vacuo to give yellow solid **2b** in 80% yield. mp 180-181 °C. ^1H NMR (500 MHz, DMSO) δ 9.93 (s, 2H), 7.79 (d, $J = 7.6$ Hz, 4H), 7.43 (d, $J = 7.6$ Hz, 4H), 4.34 (s, 4H), 4.08 (s, 4H), 2.39 (s, 6H), 1.75 (s, 6H). ^{13}C NMR (126 MHz, DMSO) δ 154.9, 143.7, 136.7, 129.7, 128.1, 84.1, 71.3, 68.0, 21.5, 15.2. HRMS (ESI-TOF) m/z : $[\text{M}+\text{Na}]^+$ calcd for $\text{C}_{28}\text{H}_{30}\text{FeN}_4\text{NaO}_4\text{S}_2$ 629.0956; Found: 629.0959.

Acknowledgements

This work was supported by the National Natural Science Foundation of China (Grant No. 21861028), Natural Science Foundation of Inner Mongolia (2017MS0206) and Grassland Talent Innovative Teams of Inner Mongolia Autonomous Region.

Supplementary data

Supplementary data (The crystal structure of compound **2a** and **2b** has been deposited at the Cambridge Crystallographic Data Centre (<http://www.ccdc.cam.ac.uk/>) with deposition number CCDC 1887250 and 1887251) associated with this article can be found in the online version, at <http://xx>.

References and notes

- 1 Nagajyoti, P. C.; Lee, K. D.; Sreekanth, T. V. M. *Environ. Chem. Lett.* **2010**, *8*,

- 199-216.
- 2 Prodi, L.; Bolletta, F.; Montalti, M.; Zaccheroni, N. *Coord. Chem. Rev.* **2000**, *205*, 59-83.
 - 3 Tchounwou, P. B.; Ayensu, W. K.; Ninashvili, N.; Sutton, D. *Environ. Toxicol.* **2003**, *18*, 149-175.
 - 4 Bost, M.; Houdart, S.; Oberli, M.; Kalonji, E.; Huneau, J.-F.; Margaritis, I. *J. Trace Elem. Med. Bio.* **2016**, *35*, 107-115.
 - 5 Kozłowski, H.; Janicka-Kłos, A.; Brasun, J.; Gaggelli, E.; Valensin, D.; Valensin, G. *Coord. Chem. Rev.* **2009**, *253*, 2665-2685.
 - 6 Kirk, K. L. In *Biochemistry of the Elemental Halogens and Inorganic Halides*; Kirk, K. L., Eds.; Plenum press, New York, 1991; Chapter Biochemistry of Inorganic Fluoride, pp 19-68.
 - 7 Kleerekoper, M. *Endocrinol. Metab. Clin. North. Am.* **1998**, *27*, 441-452.
 - 8 Geddes, C. D. *Meas. Sci. Technol.* **2001**, *12*, R53-R88.
 - 9 Kissa, E. *Clin. Chem.* **1987**, *33*, 253-255.
 - 10 Beer, P. D.; Hayes, E. J. *Coord. Chem. Rev.* **2003**, *240*, 167-189.
 - 11 Gale, P. A.; García-Garrido, S. E.; Garric, J. *Chem. Soc. Rev.* **2008**, *37*, 151-190.
 - 12 Tatum, L. A.; Su, X.; Aprahamian, I. *Acc. Chem. Res.* **2014**, *47*, 2141-2149.
 - 13 Su, X.; Aprahamian, I. *Chem. Soc. Rev.* **2014**, *43*, 1963-1981.
 - 14 Yang, Y.; Gao, C. Y.; Liu, J.; Dong D. *Anal. Methods-UK* **2016**, *8*, 2863-2871.
 - 15 Aprahamian, I. *Chem. Commun.* **2017**, *53*, 6674-6684.
 - 16 Xiang, Y.; Tong, A. J.; Jin, P. Y.; Ju, Y. *Org. Lett.* **2006**, *8*, 2863-2866.
 - 17 Liao, Z. C.; Yang, Z. Y.; Li, Y.; Wang, B. D.; Zhou, Q. X. *Dyes Pigments* **2013**, *97*, 124-128.
 - 18 Goswami, S.; Chakraborty, S.; Paul, S.; Halder, S.; Maity, A. C. *Tetrahedron Lett.* **2013**, *54*, 5075-5077.
 - 19 Zhou, L. L.; Zhang, X. H.; Wu, S. K. *Chem. Lett.* **2004**, *33*, 850-851.
 - 20 Shao, J.; Lin, H.; Yu, M.; Cai, Z. S.; Lin, H. K. *Talanta* **2008**, *74*, 1122-1125.
 - 21 Hu, S. Z.; Guo, Y.; Xu, J.; Shao, S. J. *Org. Biomol. Chem.* **2008**, *6*, 2071-2075.
 - 22 Sun, Y.; Liu, Y.; Guo, W. *Sensor Actuat. B-Chem.* **2009**, *143*, 171-176.

- 23 Fang, Y.; Zhou, Y.; Rui, Q.; Yao, C. *Organometallics* **2015**, *34*, 2962–2970.
- 24 Lakshmi, N. V.; Mandal, D.; Ghosh, S.; Prasad, E. *Chem. Eur. J.* **2014**, *20*, 9002-9011.
- 25 Mishra, S.; Dewangan, S.; Giri, S.; Mobin, S. M.; Chatterjee, S. *Eur. J. Inorg. Chem.* **2016**, *35*, 5485-5496.
- 26 Ling, L.; Hu, J. F.; Huo, Y. H.; Zhang, H. *Tetrahedron* **2017**, *73*, 86-97.
- 27 Yang M. H.; Thirupathi P.; Lee K. H. *Org. Lett.* **2011**, *13*, 5028-5031.
- 28 Shortreed, M.; Kopelman, R.; Kuhn, M.; Hoyland, B. *Anal. Chem.* **1996**, *68*, 1414-1418.

Highlights:

- New and simple ferrocenyl hydrazone chemosensors were designed and synthesized by using an easy way.
- Chemosensors **2a** and **2b** has proved to be a versatile ion recognition ability for both cations and anions.
- Hg^{2+} , Cu^{2+} and F^- ions are detectable by using colorimetric, optical (UV-vis) and electrochemical signals.
- The color of the solution containing chemosensors **2a** and **2b** changed from pale yellow to red upon the addition of Hg^{2+} , while the color changed to yellow green when Cu^{2+} ions were added.